ELSEVIER

A low-Reynolds-number, four-equation heat transfer model for turbulent separated and reattaching flows

Gwang Hoon Rhee and Hyung Jin Sung
Department of Mechanical Engineering, Korea Advanced Institute of Science and Technology, Kusong-dong, Yusong-ku, Taejon, South Korea

An algebraic heat flux model is applied to predict turbulent heat transfer in separated and reattaching flows. Based on the prior low-Reynolds-number $k-\varepsilon$ model of Park and Sung (1995), an improved version of the nonequilibrium heat transfer model is developed. The model performance is examined by solving the equations of the temperature variance k_θ and its dissipation rate ε_θ, together with the equations of k and ε. In the present model, the near-wall limiting behaviour close to the wall and the nonequilibrium effect away from the wall are incorporated. A tensor eddy-diffusivity is obtained to implement the orientation of mean temperature gradient in separated and reattaching flows. The validation of the model is applied to the turbulent flow over a backward facing step. The predictions of the present model are cross-checked with the existing measurements and direct numerical simulation (DNS) data. The model performance is shown to be generally satisfactory.

Keywords: low-Reynolds-number heat transfer model; tubulent separated and reattaching flows

Introduction

Comprehensive knowledge of flow structure is essential to analyze the attendant heat transport phenomena. As a multipronged attack on the problem of turbulent flow and heat transfer processes in separated and reattaching flows, an improved version of the nonlinear low-Reynolds-number $k-\varepsilon$ model has been developed by Park and Sung (1995). In their model, the limiting near-wall behavior and nonlinear Reynolds stress representations were incorporated. The main emphasis was placed on the adoption of $R_y(\equiv k^{1/2}y/\nu)$ instead of $y^+(\equiv u_\tau y/\nu)$ in the low-Reynolds-number model to avoid the difficulties at the separation and reattachment points ($u_\tau = 0$). The nonequilibrium effect was also taken into account to describe recirculating flows away from the wall. The model performance was shown to be generally satisfactory. Based on the aforementioned fluid flow model, efforts are now directed toward extending the model to thermal field computation.

A literature survey reveals that most of the studies on heat transfer in separated and reattaching flows have contained mainly mean heat transfer rates and very little fluid dynamic data (Fletcher et al. 1974; Aung and Watkins 1978; Aung and Goldstein 1972). However, in order to understand the dynamic characteristics of turbulent heat transfer, turbulence quantities are more informative. Contrary to the aforementioned research, studies on the combined heat transfer and fluid dynamic measurements in turbulent separated and reattaching flows are relatively scarce (Vogel and Eaton 1985). Combined heat transfer and fluid dynamic measurements downstream of a backward-facing step have been made by Vogel and Eaton, in which the heat transfer data coupled with temperature and velocity profiles were provided to scrutinize the mechanisms of controlling the heat transfer rate in reattaching flows.

In contrast to the preceding rare experiments, there have been many numerical thermal field computations in turbulent separated and reattaching flows (Ciofalo and Collins 1989; Chieng and Launder 1980; Dutta and Acharya 1993; Arman and Rabas 1994). Most computations cited in the literature are implemented by using the $k-\varepsilon$ model. Conventionally, turbulent heat transfer is simulated by employing the turbulent Prandtl number Pr_t, in which the eddy-diffusivity of heat α_t is prescribed through the known eddy-viscosity ν_t. This assumption; i.e., Pr_t-constant, satisfies Pope's linear superposition principle of scalars in turbulent flows (Pope 1983). However, it is revealed that there are no universal values of Pr_t even in simple attaching flows (Reynolds 1975; Antonia 1980). Furthermore, it is expected that the values in separated and reattaching flows differ substantially from those in an ordinary boundary layer.

As pointed out by Rogers et al. (1989), simple gradient–transport-type models work well for predicting the scalar heat flux in homogeneous flows, where the simple model is represented as $-\overline{u_i\theta} = \alpha_t \partial T/\partial x_i$. However, this model is inadequate to predict convective heat transfer in separated and reattaching flows. This is because the scalar heat fluxes are no longer aligned with the mean temperature gradiants. Additionally, the magnitude of the flux component down the gradient varies substantially, depending on the direction of the imposed mean temperature gradient. A

Address reprint requests to Dr. H. J. Sung, Department of Mechanical Engineering, Korea Advanced Institute of Science and Technology, 373-1 Kusong-dong, Yusong-ku, Taejon, 305-701, South Korea.

Received 10 March 1996; accepted 15 October 1996

Int. J. Heat and Fluid Flow 18:38–44, 1997

655 Avenue of the Americas, New York, NY 10010

0142-727X/97/$17.00
PII S0142-727X(96)00137-2

tensor eddy-diffusivity is obtained to implement the orientation of mean temperature gradient with respect to the mean temperature.

To analyze heat transfer problems numerically in separated and reattaching flows, an algebraic heat flux model (Rogers et al. 1989; Gibson and Launder 1976) is employed in the present study. In the recirculation region, it is known that the effect of nonequilibrium away from the wall becomes dominant. This means that the production of turbulent energy P_k is not balanced with its dissipation ε; i.e., $P_k/\varepsilon \neq 1$. To address this point, the nonequilibrium effect of velocity field (P_k/ε) as well as the thermal nonequilibrium effect $(P_\theta/\varepsilon_\theta)$ are incorporated in the present algebraic heat flux model. The eddy-diffusivity tensor is then obtained by solving the two equations of temperature variance (k_θ) and its dissipation rates (ε_θ), together with the equations of k and ε. Correct near-wall limiting behavior is a prerequisite to accurate prediction of convective heat transport in separated and reattaching flows. A wall damping function f_λ is adopted in the present algebraic heat flux model, where f_λ satisfies the wall limiting behavior.

Turbulence model for velocity field

To evaluate the turbulent heat transfer in separated and reattaching flows accurately, the prediction of flow fields with sufficient accuracy should come first. As mentioned in the introduction, an improved version of the nonlinear low-Reynolds number k–ε model for turbulent separated and reattaching flows has been developed by Park and Sung (1995). In this section, the model is briefly summarized. Details regarding the model formulations are compiled in Park and Sung. For a stationary, incompressible flow field, the governing equations are in line with the equations of the turbulent kinetic energy k and its dissipation rate ε. These equations are written in Cartesian tensor notations as

$$\frac{\partial U_i}{\partial x_i} = 0 \tag{1}$$

$$U_j\frac{\partial U_i}{\partial x_j} = -\frac{\partial P}{\partial x_i} + \frac{\partial}{\partial x_j}\left(\nu\frac{\partial U_i}{\partial x_j} - \overline{u_i u_j}\right) \tag{2}$$

$$U_j\frac{\partial k}{\partial x_j} = \frac{\partial}{\partial x_j}\left[\left(\nu + f_t\frac{\nu_t}{\sigma_k}\right)\frac{\partial k}{\partial x_j}\right] + P_k - \varepsilon \tag{3}$$

$$U_j\frac{\partial \varepsilon}{\partial x_j} = \frac{\partial}{\partial x_j}\left[\left(\nu + f_t\frac{\nu_t}{\sigma_\varepsilon}\right)\frac{\partial \varepsilon}{\partial x_j}\right] + C^*_{\varepsilon_1}P_k\frac{\varepsilon}{k} - C_{\varepsilon_2}f_2\frac{\varepsilon^2}{k} + \left(C_1\nu\nu_t S^{*2}_{,j} + C_2\nu\frac{k}{\varepsilon}k_{,j}S^*S^*_{,j}\right)f_{w_1} \tag{4}$$

$$-\overline{u_i u_j} = 2\nu_t S_{ij} - \frac{2}{3}k\delta_{ij} + C_{\alpha_1}\nu_t\frac{k}{\varepsilon}\left(S_{im}S_{mj} - \frac{1}{3}S_{mn}S_{mn}\delta_{ij}\right) + C_{\alpha_2}\nu_t\frac{k}{\varepsilon}(\omega_{im}S_{mj} - \omega_{jm}S_{mi}) \tag{5}$$

$$\nu_t = C_\mu f_\mu\frac{k^2}{\varepsilon} \tag{6}$$

$$f_{\mu_1} = (1 - f_{w_1})(1 + 10f_{w_1}/R_t^{1.25}) \tag{7}$$

$$f_{\mu_2} = C_{\mu_1}\frac{(C_{\mu_2} + C_{\mu_3}P_k/\varepsilon)}{(C_{\mu_2} + P_k/\varepsilon)^2} \tag{8}$$

The unknown Reynolds stress $-\overline{u_i u_j}$ is expanded up to the second-order term in a nonlinear k–ε model (Rubinstein and Barton 1990; Speziale 1991). The nonequilibrium effect (P_k/ε) is incorporated into $C^*_{\varepsilon_1}$ which has the form $C^*_{\varepsilon_1} = C_{\varepsilon_1}(0.95 + 0.05P_k/\varepsilon)$. S^* is a modified strain rate parameter, $S^* = 2.75\sqrt{\nu\varepsilon}/(\nu + \nu_t)$. The model constant C_1, C_2, C_{ε_1}, and C_{ε_2} are set as $C_1 = 1.0$, $C_2 = 0.006$, $C_{\varepsilon_1} = 1.45$ and $C_{\varepsilon_2} = 1.9$, respectively. C_{α_1}, C_{α_2}, and C_μ are the model constants ($C_{\alpha_1} = 0.6$, $C_{\alpha_2} = 0.4$ and $C_\mu = 0.09$). The damping function f_μ is expressed as $f_\mu = f_{\mu_1}f_{\mu_2}$, which reflects the effect of wall-proximity (f_{μ_1}) and the nonequilibrium effect away from the wall (f_{μ_2}).

Notation

c	specific heat
C_f	mean skin friction coefficient
$C_\mu, C_{\varepsilon_1}, C_{\varepsilon_2}$	model constants
$f_\mu, f_1, f_2, f_\lambda$	model functions
H	height of backward-facing step
h	heat transfer coefficient $[= q_w/(T_w - T_\infty)]$
k	turbulent kinetic energy
k_θ	temperature variance
Pr	Prandtl number $(= \alpha/\nu)$
Pr_t	turbulent Prandtl number $(= \alpha_t/\nu_t)$
P_k	production of turbulent energy $(= -\overline{u_i u_j}\,\partial U_i/\partial x_j)$
P_θ	production of temperature variance $(= -\overline{u_i\theta}\,\partial T/\partial x_i)$
R	time-scale ratio $[= (k_\theta/\varepsilon_\theta)/(k/\varepsilon)]$
R_t	turbulent Reynolds number $(= k^2/\nu\varepsilon)$
S_{ij}	strain rate tensor $[= 0.5(U_{i,j} + U_{j,i})]$
St	Stanton number $(= h/U\rho c)$
T	mean temperature
X_R	reattachment length

Greek

α, α_t	thermal diffusivity and thermal eddy-diffusivity
δ	boundary-layer thickness
δ_θ	thermal boundary-layer thickness
ε	dissipation rate of turbulent energy
ε_θ	dissipation rate of temperature variance
ν, ν_t	kinematic viscosity and eddy-viscosity
ρ	density
$\sigma_k, \sigma_\varepsilon, \sigma_h, \sigma_\phi$	model constants of turbulent diffusion
ω_{ij}	vorticity tensor $[= 0.5(U_{i,j} - U_{j,i})]$

Turbulence model for thermal field

Governing equations

The governing equations for turbulent heat transports are expressed as (Abe et al. 1995),

$$U_j\frac{\partial T}{\partial x_j}=\frac{\partial}{\partial x_j}\left[\alpha\frac{\partial T}{\partial x_j}-\overline{u_j\theta}\right] \tag{9}$$

$$U_j\frac{\partial k_\theta}{\partial x_j}=\frac{\partial}{\partial x_j}\left[\left(\alpha+f_h\frac{\alpha_t}{\sigma_h}\right)\frac{\partial k_\theta}{\partial x_j}\right]+P_\theta-\varepsilon_\theta \tag{10}$$

$$U_j\frac{\partial \varepsilon_\theta}{\partial x_j}=\frac{\partial}{\partial x_j}\left[\left(\nu+f_h\frac{\alpha_t}{\sigma_\phi}\right)\frac{\partial \varepsilon_\theta}{\partial x_j}\right]-C_{p_1}\frac{\varepsilon_\theta}{k_\theta}\overline{u_j\theta}\frac{\partial T}{\partial x_j}$$
$$+C_{p_2}\frac{\varepsilon_\theta}{k}\overline{u_iu_j}\frac{\partial U_i}{\partial x_j}-C_{D_1}f_{D_1}\frac{\varepsilon\theta^2}{k_\theta}-C_{D_2}f_{D_2}\frac{\varepsilon\varepsilon_\theta}{k} \tag{11}$$

As shown above, the eddy-diffusivity for heat α_t in Equations 10 and 11 is obtained by introducing the constant turbulent Prandtl number $\mathrm{Pr}_t=\alpha_t/\nu_t=0.9$. f_h is the model function for turbulent diffusion. It is revealed that the roles of turbulent diffusion are substantial in the near-wall region (Abe et al. 1995). In the present study, the following model is thus proposed as $f_h=1+3.03\exp-\sqrt{R_t}/15]$, which is modified from the f_t function in velocity field (Park and Sung 1995). P_θ represents the rate of production of the temperature fluctuations, $P_\theta=-\overline{u_i\theta}\partial T/\partial x_i$.

Algebraic formulation for $\overline{u_i\theta}$

The turbulent heat flux components $\overline{u_i\theta}$ are evaluated by the following algebraic model. The basic physical model has been developed by other (Gibson and Launder 1976) for the restricted case where the ratio of turbulence-energy production and dissipation rate is equal throughout the flow; i.e., $P_k/\varepsilon=1$. The present work extends the treatment to more realistic flows; i.e., separated and reattaching flows, in which the ratio of P_k/ε varies from point to point.

The algebraic formula for the turbulent heat fluxes is expressed as (Rogers et al. 1989)

$$\overline{u_i\theta}=\frac{2kk_\theta(P_{i\theta}+\phi_{i\theta})}{k_\theta(P_k-\varepsilon)+k(P_\theta-\varepsilon_\theta)} \tag{12}$$

where $P_{i\theta}$ denotes the production rates of $\overline{u_iu_j}$ and $\overline{u_i\theta}$, respectively; i.e., $P_{i\theta}=-\overline{u_iu_j}\partial T/\partial x_j-\overline{u_j\theta}\partial U_i/\partial x_j$. $\phi_{i\theta}$ represents the pressure–temperature-gradient correlation, $\phi_{i\theta}=\overline{p\partial\theta/\partial x_i}$ (Gibson and Launder 1976). Following Gibson and Launder (1976; 1978), $\phi_{i\theta}$ is modeled as

$$\phi_{i\theta}=C_{1\theta}\frac{\varepsilon}{k}\overline{u_i\theta}-C_{2\theta}P_{i\theta} \tag{13}$$

Here, $C_{1\theta}$ and $C_{2\theta}$ are the model constants ($C_{1\theta}=3.0$ and $C_{2\theta}=0.33$). The direct substitution of Equation 13 into Equation 12 yields the following nondimensional expression for $b_{i\theta}$

$$b_{i\theta}=-\left(b_{ij}+\frac{\delta_{ij}}{3}\right)\frac{\partial T^*}{\partial x_j}-b_{j\theta}S^*_{ij} \tag{14}$$

in which $b_{i\theta}$ is defined as $b_{i\theta}\equiv\overline{u_i\theta}/2\sqrt{kk_\theta}$, and b_{ij} denotes the anisotropic tensor of turbulence $b_{ij}\equiv\overline{u_iu_j}/2k-\delta_{ij}/3$. The dimensionless rescaled variables in Equation 14 are

$$\frac{\partial T^*}{\partial x_j}=2g_\theta\tau(1-C_{2\theta})\sqrt{\frac{k}{k_\theta}}\frac{\partial T}{\partial x_j} \tag{15}$$

$$S^*_{ij}=g_\theta\tau(1-C_{2\theta})S_{ij} \tag{16}$$

In the above, the variable g_θ is a function of both the effect of nonequilibrium of velocity field (P_k/ε) and that of thermal field ($P_\theta/\varepsilon_\theta$):

$$g_\theta=\{C_{1\theta}+P_k/\varepsilon-1+(P_\theta/\varepsilon_\theta-1)/R\}^{-1} \tag{17}$$

where R represents the ratio of the characteristic decay times for the turbulent temperature and velocity fields, $R\equiv(k_\theta/\varepsilon_\theta)/(k/\varepsilon)$. τ is the velocity time-scale $\tau=k/\varepsilon$. It is noted that, if the local equilibrium states are taken as equal ($P_k/\varepsilon=1$ and $P_\theta/\varepsilon_\theta=1$), the present model would be the same as the prior general algebraic models except for the wall treatment of the pressure–velocity strain term (Gibson and Launder 1978).

In matrix form, Equation 14 can be written as follows:

$$\begin{bmatrix}S^*_{11}+1 & S^*_{12} & S^*_{13}\\ S^*_{22} & S^*_{22}+1 & S^*_{23}\\ S^*_{31} & S^*_{32} & S^*_{33}+1\end{bmatrix}\begin{bmatrix}b_{1\theta}\\ b_{2\theta}\\ b_{3\theta}\end{bmatrix}$$
$$=-\begin{bmatrix}b_{11}+\frac{1}{3} & b_{12} & b_{13}\\ b_{21} & b_{22}+\frac{1}{3} & b_{23}\\ b_{31} & b_{32} & b_{33}+\frac{1}{3}\end{bmatrix}\begin{bmatrix}\frac{\partial T^*}{\partial x}\\ \frac{\partial T^*}{\partial y}\\ \frac{\partial T^*}{\partial z}\end{bmatrix} \tag{18}$$

If we now limit our attention to two-dimensional (2-D) formulation, Equation 18 then yields the following formulas for the heat flux components

$$-\overline{u\theta}=C_gf_\lambda A_\theta\left\{\begin{array}{l}[\overline{u^2}(A_\theta S_{22}+1)-\overline{uv}A_\theta S_{12}]\frac{\partial T}{\partial x}\\ +[-\overline{uv}(A_\theta S_{22}+1)+\overline{v^2}A_\theta S_{12}]\frac{\partial T}{\partial y}\end{array}\right\} \tag{19}$$

$$-\overline{v\theta}=C_gf_\lambda A_\theta\left\{\begin{array}{l}[\overline{u^2}A_\theta S_{21}-\overline{uv}(A_\theta S_{11}+1)]\frac{\partial T}{\partial x}\\ +[-\overline{uv}A_\theta S_{21}+\overline{v^2}(A_\theta S_{11}+1)]\frac{\partial T}{\partial y}\end{array}\right\} \tag{20}$$

Here, the model constant C_g is set as $C_g=0.6$, which is modeled from the reciprocal of the determinant of Equation 19. f_λ represents the well-damping function to incorporate the near-wall effect. The expression of A_θ in Equations 19 and 20 is given as $A_\theta=g_\theta\tau(1-C_{2\theta})$.

Formulation of f_λ

For accurate prediction of heat transfer in separated and reattaching flows, it is highly important to reproduce the near-wall limiting behavior correctly. In the near-wall region, the asymptotic behaviors maintain the following relations $-\overline{v\theta}\propto y^3$, $\partial T/\partial y\propto y^0$, $A_\theta\propto y^2-\overline{uv}\propto y^3$, $-\overline{v^2}\propto y^4$ and $S_{12}\propto y^0$ as $y\to 0$. In a manner similar to the wall-damping formulation in flow fields, f_λ

is formulated as

$$f_\lambda = (1 - T_{w_1})(1 + 10T_{w_1}/\mathrm{R}_t^{1.25}) \tag{21}$$

$$T_{w_1} = \exp\left[-\left(\frac{\mathrm{R}_y}{80}\right)^2 \mathrm{Pr}^{1.5}\right] \tag{22}$$

where Pr denotes the Prandtl number. R_t and R_y stand for, respectively, the turbulent Reynolds number $\mathrm{R}_t = k/(\nu\varepsilon)$ and $\mathrm{R}_y = \sqrt{k}y/\nu$. The wall-reflection function T_{w_1} represents the effect of wall-proximity in the near-wall region. As mentioned earlier, f_λ is found to satisfy the wall limiting behavior; i.e., $f_\lambda \propto y^{-3}$.

Modeling of the ε_θ-equation

The ε_θ-equation can be modeled in a way similar to the prior models (Nagano and Kim 1988; Youssef et al. 1992; Abe et al. 1995):

$$U_j\frac{\partial \varepsilon_\theta}{\partial x_j} = \frac{\partial}{\partial x_j}\left[\left(\nu + f_h\frac{\alpha_t}{\sigma_\phi}\right)\frac{\partial \varepsilon_\theta}{\partial x_j}\right] - C_{p_1}\frac{\varepsilon_\theta^2}{k_\theta}\overline{u_j\theta}\frac{\partial T}{\partial x_j}$$

$$- C_{p_2}\frac{\varepsilon_\theta}{k}\overline{u_iu_j}\frac{\partial U_i}{\partial x_j} - C_{D_1}f_{D_1}\frac{\varepsilon_\theta^2}{k_\theta} - C_{D_2}f_{D_2}\frac{\varepsilon\varepsilon_\theta}{k} \tag{23}$$

In the above equation, the model constants C_{p_1} and C_{p_2} for the production terms are determined by fitting the DNS data (Kim and Moin 1987; Kasagi et al. 1992); i.e., $C_{p_1} = 0.9$ and $C_{p_2} = 0.72$, respectively.

The limiting behavior of wall turbulence should be taken into account to balance the ε_0 budget in the near-wall region. It is known that the near-wall asymptotic behavior of wall turbulence is derived as: $k \sim y^2$ and $k_\theta \sim y^2$. To avoid the singularities in the ε_0-equation near the wall, the following relations are required; i.e., $f_{D_1} \propto y^2$ and $f_{D_2} \propto y^2$. Thus, f_{D_1} is modeled as $f_{D_1} = 1 - \exp(-\mathrm{R}_y/8.1)$. From the decay law of homogeneous turbulence (Nagano and Kim 1988), the f_{D_2} model function can be modeled as

$$f_{D_2} = \frac{C_{\varepsilon_2}f_2 - 1}{C_{D_2}}f_{D_W} \tag{24}$$

with the relations $C_{D_1}f_{D_1} = 1$ and $C_{D_2}f_{D_2} = C_{\varepsilon_2}f_2 - 1$. The model constants can be set as $C_{D_1} = 1$ and $C_{D_2} = 0.9$ (Nagano and Kim 1988). In Equation 24, the leading term; i.e., $(C_{\varepsilon_2} - 1)/C_{D_2}$ represents the effect of free-turbulence, and f_{D_W} denotes the wall-proximity near the wall. f_{D_W} is obtained by fitting the DNS data (Kim and Moin 1987; Kasagi et al. 1992); i.e., $f_{D_W} = 1 - \exp(-R_y/8.1)$. The f_{D_2} function satisfies the limiting behavior correctly, $f_{D_2} \propto y^2$.

Results and discussion

The main aim of the present model is to predict turbulent thermal quantities in separated and reattaching flows. However, it is important to ascertain the generality and accuracy of the present model to an attached boundary layer. Because turbulence quantities are available from DNS data (Kim and Moin 1987; Kasagi et al. 1992), first we have applied the model to a fully developed channel flow with two typical boundary conditions; i.e., with a uniform wall temperature and a uniform heat flux. Next, the proposed model is tested for the combined heat and fluid flow over a backward-facing flow. This flow configuration is frequently used for benchmarking the performance of turbulence models for separated and reattaching flows. The model predictions are compared with the experimental data of Vogel and Eaton (1985) for a backward-facing step flow.

Model performance in a channel flow

The numerical scheme used is a well-established finite-volume method. The boundary conditions are: $U = k = k_\theta = 0$, $\varepsilon = \nu\partial^2 k/\partial y^2$, $\varepsilon_\theta = \alpha\partial^2 k_\theta/\partial y^2$, T_w = constant or q_w = constant at the wall; $\partial U/\partial y = \partial k/\partial y = \partial\varepsilon/\partial y = \partial T/\partial y = \partial k_\theta/\partial y = 0$ at the central axis. To obtain the grid-independent solutions, we need 101 nonuniform grid points in the direction normal to the wall. The grid convergence was checked, and the outcome of these tests was found to be satisfactory.

The predicted profiles of temperature T^+ by the present model are exhibited in Figure 1 under two different wall thermal conditions. The selected Reynolds numbers are $\mathrm{Re}_\tau = 150$ and 180, for which the DNS data exist. The model predictions by Abe et al. (1995) (hereafter referred to as AKN model) are also displayed for comparisons. The AKN model is recently developed for predicting fluid flow and heat transfer in separated and reattaching flows. As seen in Figure 1, the present model shows good predictions with DNS data for both the uniform wall temperature and uniform wall heat flux conditions (Kim and Moin 1987; Kasagi et al. 1992), while the AKN model slightly underpredicts in the outer region ($y^+ > 50$).

The predicted profiles of turbulent heat flux $\overline{v\theta}^+$ in the near-wall region are shown in Figure 2. The DNS data of Kasagi et al. (1992) with the uniform wall heat flux condition (q_w = constant) is included for comparision. Both the present model and the AKN model provide good agreements with DNS data. The normalized profiles of temperature variance k_θ^+ are displayed in Figure 3. The present model predictions show excellent agreements with DNS data, however, the predicted results by the AKN model are slightly underpredicted. The near-wall behavior of k_θ^+ are also plotted in Figure 4 with a logarithmic scale. The agreement with DNS data in the near-wall region is good by the present model.

Figure 5 compares the budget of k_θ-equation with the DNS data. As is evident, the present model follows the DNS data well. Although a little discrepancy is exhibited near the region $y^+ \approx 10$, the present model reproduces the near-wall behavior better than the AKN model. The near-wall behavior of ε_θ^+ is shown in

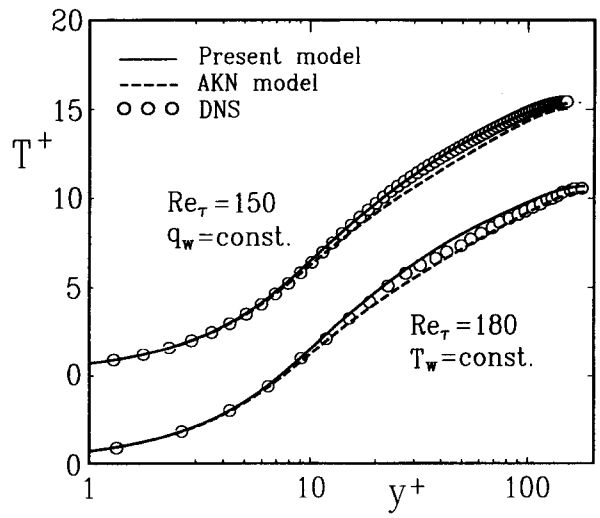

Figure 1 Comparison of the predicted T with DNS data

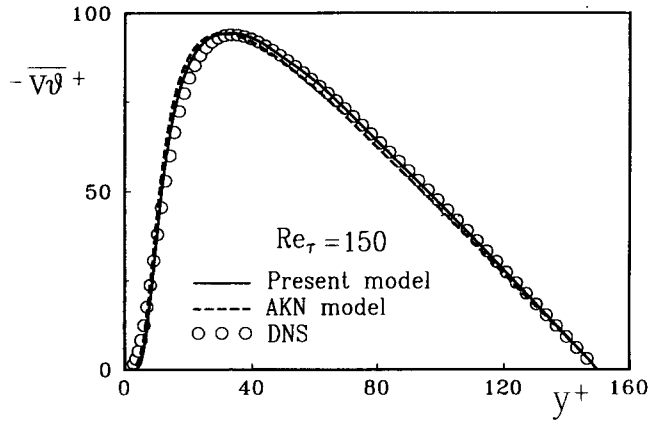

Figure 2 Comparison of the predicted $-\overline{vq}$ with DNS data

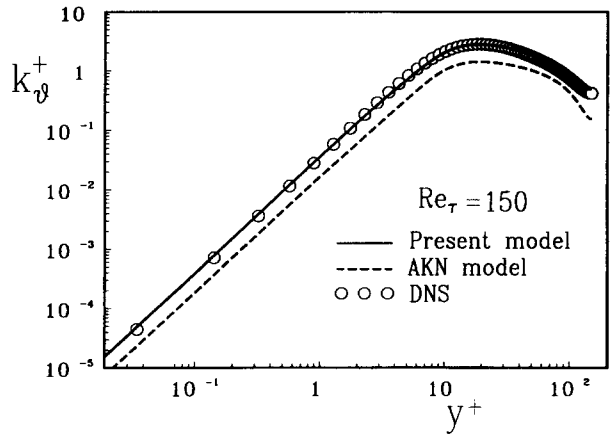

Figure 4 Near-wall behavior of the predicted k_θ

Figure 6. As compared with the prior profile of ε in velocity fields by Park and Sung (1995), the predicted ε_θ^+ profile is seen to be less accurate. However, the present model follows the wall behavior fairly well.

Model performance in separated and reattaching flows

As mentioned earlier, a benchmarking experiment is selected to test the present model for separated and reattaching flows; a backward-facing step flow (Vogel and Eaton 1985). Before proceeding further, the numerical procedure and boundary conditions for these elliptic computations are briefly summarized in the following. The finite-difference equations are discretized using the hybrid linear parabolic approximation (HLPA) scheme with second-order accuracy. A nonstaggered variable arrangement is adopted with the momentum interpolation technique to avoid the pressure–velocity decoupling. The coupling between pressure and velocity is achieved by the SIMPLEC prediction-corrector algorithm, which is an improved version of the SIMPLE algorithm. The set of discretized linear algebraic equations is solved by a strongly implicit procedure(SIP). The boundary conditions are: $U = V = k = k_\theta = 0$, $\varepsilon = \nu\partial^2 k/\partial n^2$, $\varepsilon_\theta = \alpha\partial^2 k_\theta/\partial n^2$, $\partial P/\partial n = 0$ and q_w = constant at the bottom wall surface. The inlet conditions are given from the experimental conditions together with $\partial P/\partial n = 0$. The Neuman conditions are applied at the outlet. The computations were done on a CRAY-YMP supercomputer. Convergence was declared when the maximum normalized sum of absolute residual sources over all the computational nodes was less than 10^{-4}. Several trial calculations were repeated to monitor the sensitivity of the results to grid resolution. The nonorthogonal finer-resolution grid systems were (201 × 121), where the grid points were crowded near the wall boundaries and clustered in the recirculating region.

As a validation of flow-field computation, the wall shear stress coefficient C_f is exhibited in Figure 7, which is closely related to the prediction of turbulent heat transfer near the wall. The predicted C_f is plotted against a nondimensional streamwise coordinate $X^* = (X - X_R)/X_R$, together with the experimental data of Vogel and Eaton (1985). Here, X_R represents the reattachment length. The step-height Reynolds number is Re_H = 28,000. It is seen that the present model prediction in the recirculation region is in better agreement with the experiment than the AKN model prediction.

The Stanton number St profiles are displayed in Figure 8 by using the same coordinate X^*. The Stanton number profiles by employing the turbulent Prandtl number $Pr_t = 0.9$, without solving the $k_\theta, \varepsilon_\theta$ equations, are also plotted in Figure 8. Comparison between the predicted results and the experimental data indicates that the present model prediction is in overall better agreement with the experiment. The predicted results of $Pr_t = 0.9$

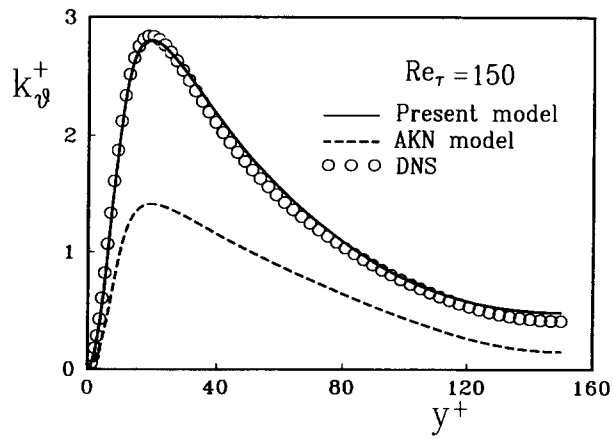

Figure 3 Comparison of the predicted k_θ with DNS data

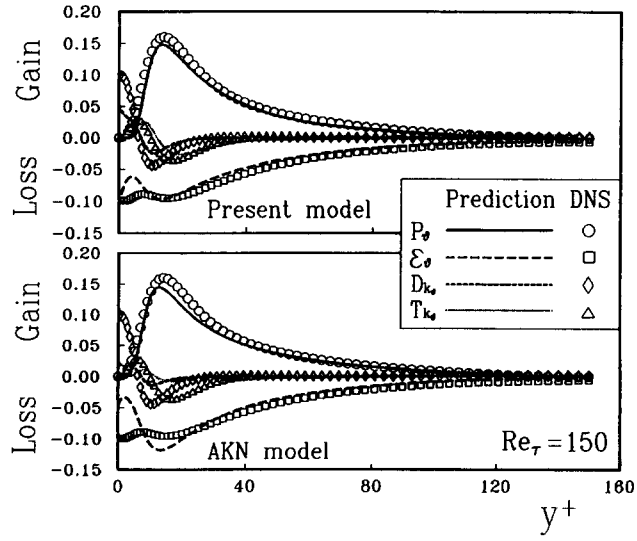

Figure 5 Comparison of the budget of k_θ-equation with DNS data

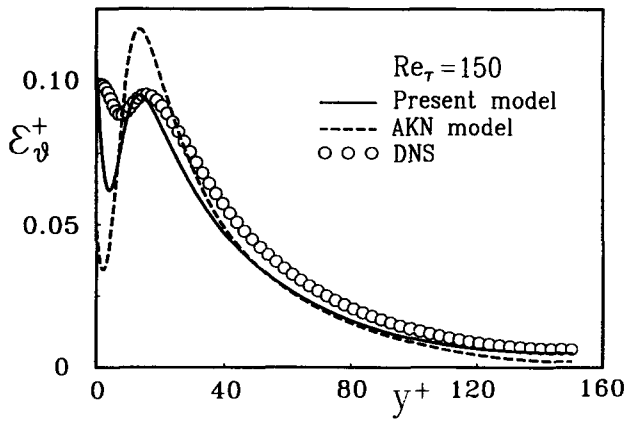

Figure 6 Comparison of the predicted ε_θ with DNS data

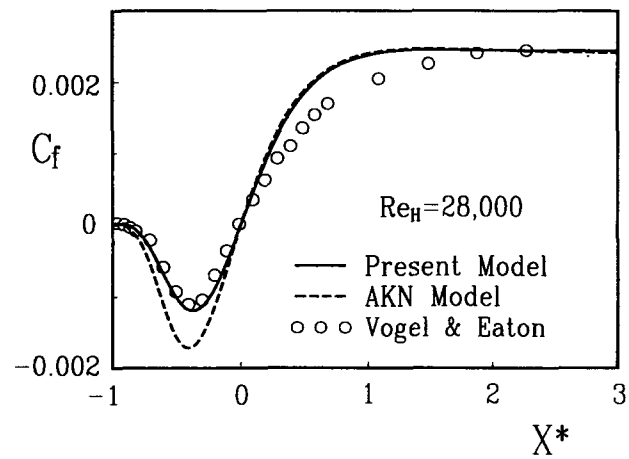

Figure 7 Comparison of the predicted C_f with experimental data

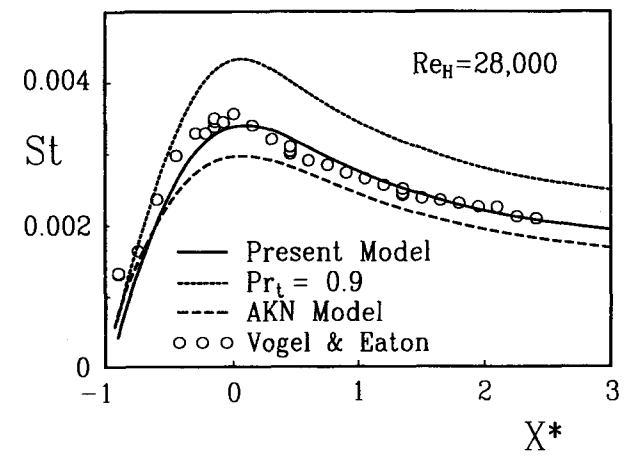

Figure 8 Comparison of the predicted St with experimental data

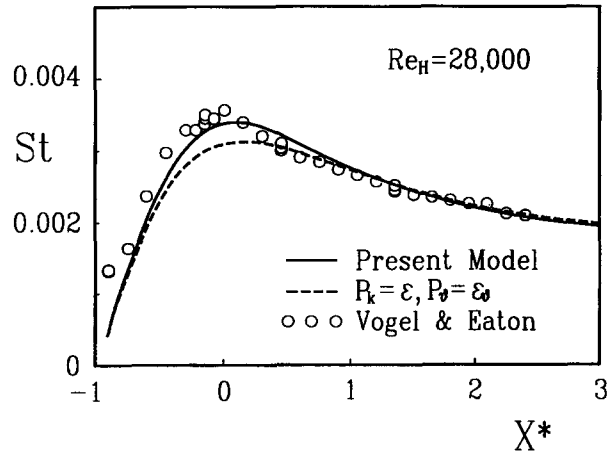

Figure 9 Nonequilibrium effect on Stanton number

is overpredicted near the recirculation region, while the AKN model slightly underpredicts. However, all of the Stanton number profiles have the same general features; i.e., the peak heat transfer rates occurs near the reattachment region ($X^* = 0$) and there is a low heat transfer in the recirculation region. The heat transfer coefficient recovers fairly rapidly to flat-plate behavior downstream of reattachment (Vogel and Eaton 1985).

Comparisons are extended to the nonequilibrium effects on the Stanton number profiles in Figure 9. The results of the local equilibrium state ($P_k = \varepsilon$ and $P_\theta = \varepsilon_\theta$) are also displayed with the dashed line. As expected, the consideration of the nonequilibrium effects on St is important in the recirculation region. In particular, the discrepancy near the reattachment region ($X^* \approx 0$) is significant. It is seen that the present computed results are in excellent agreement with the experiment.

The profiles of turbulent heat flux ($\overline{v\theta}^+$) near the recirculation region ($-0.7 \leq X^* \leq 0.5$) are shown in Figure 10. The step height Reynolds number is $Re_H = 13{,}000$ and $\delta/H = 1.1$, respectively. As can be seen, rather poor agreement is obtained between the predicted results and the experiment (Vogel and Eaton 1985). Moreover, the deviation is amplified near the wall region. This inadequate prediction may be attributable to the fact of incompleteness of the present model. On the other hand, as stressed by Vogel and Eaton, the fall off of the turbulent transport approaching the wall may be exaggerated due to the constraint of their measurement technique. However, the overall trends between them are generally consistent. It is seen that the change near the step is representative of the shift in the turbu-

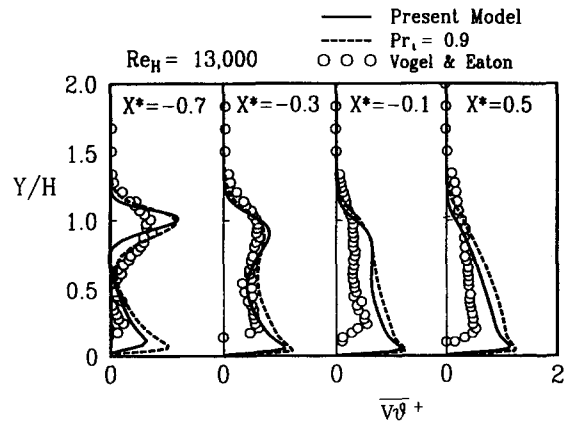

Figure 10 Comparison of the predicted $\overline{v\theta}$ with experimental data

lent transport between a free shear layer and a wall-boundary flow. At the position downstream of one half reattachment ($X^* = 0.5$), the profile is very similar to that found on a flat plate; i.e., $\overline{v\theta}^+$ highest near the wall, dropping to zero in the free stream.

Based on the wealth of numerical results, it is useful to visualize the contour plot of $R = (k_\theta/\varepsilon_\theta)/(k/\varepsilon)$ in Figure 11. The time-scale ratio is defined by the ratio of the time-scale of energy containing eddies in the thermal field ($k_\theta/\varepsilon_\theta$) to that in a velocity field (k/ε). Because turbulent mixing in the separated free-shear layer is so strong, the velocity time-scale (k/ε) becomes then very small. In contrast, the thermal time-scale ($k_\theta/\varepsilon_\theta$) is relatively large from the computation. This shows that R is very large along the separated free-shear layer.

Conclusion

A low-Reynolds number four-equation heat transfer model has been developed for predicting heat transfer in turbulent separated and reattaching flows. The limiting near-wall behavior close to the wall and the nonequilibrium effect in the recirculating region away from the wall were fully considered.

The wall-limiting behaviour of the ε_θ-equation was also incorporated. In the first, the present model was tested against the DNS data of a fully developed channel flow with a uniform wall temperature and a uniform heat flux. The near-wall behaviors of k_θ and ε_θ were reproduced fairly well. Next, the validation was extended to the flow over a backward-facing step. In testing the backward-facing step flow, the predicted results of wall shear stress coefficient C_f and Stanton number St were shown to be in good agreement with the relevant experiment. It was revealed that the present model prediction is in overall better agreement with the experiment than the case of $Pr_t = 0.9$. Furthermore, the nonequilibrium effects on St were shown to be significant. Relatively poor agreement was obtained for the predictions of turbulent heat flux. However, the overall trends were generally satisfactory. From the contour plot of R, valuable informations could be extracted.

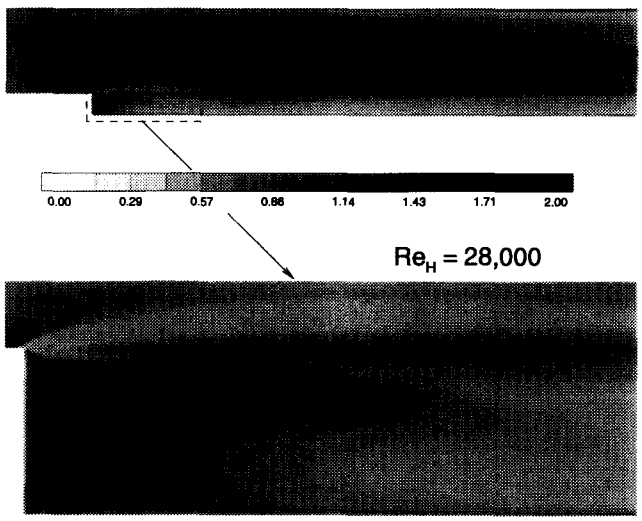

Figure 11 Contour plot of R in a backward-facing step flow

References

Abe, K., Kondoh, T., and Nagano, Y. 1995. A new turbulence model for predicting fluid flow and heat transfer in separating and reattaching flows—II. Thermal field calculations. *Int. J. Mass Transfer*, **38**, 467–481

Antonia, R. A. 1980. Behavior of the turbulent Prandtl number near the wall. *Int. J. Heat Mass Transfer*, **23**, 906–908

Arman, B. and Rabas, T. J. 1994. Two-layer-model predictions of heat transfer inside enhanced tubes. *Numer. Heat Transfer, A*, **25**, 721–741

Aung, W. and Goldstein, R. J. 1972. Heat transfer in separated flow downstream of a rearward-facing step. *Israel J. Tech.*, 35–41

Aung, W. and Watkins, C. B. 1978. Heat transfer mechanisms in separated forced convection. *Proc. NATO Institute on Turbulent Forced Convection in Channels and Bundles: Theory and Applications to Heat Exchangers*, Turkey

Chieng, C. C. and Launder B. E. 1980. On the calculation of turbulent heat transport downstream from an abrupt pipe expansion. *Numer. Heat Transfer*, **3**, 189–207

Ciofalo, M. and Collins, M. W. 1989. k–ε predictions of heat transfer in turbulent recirculating flows using an improved wall treatment. *Numer. Heat Transfer, B*, **15**, 21–47

Dutta, S. and Acharya, S. 1993. Heat transfer and flow past a backstep with the nonlinear k–ε turbulence model and the modified k–ε turbulence model. *Numer. Heat Transfer, A* **23**, 281–301

Fletcher, L. S., Briggs, D. G., and Page, R. H. 1974. Heat transfer in separated and reattaching flows: An annotated review. *Israel J. Tech.*, **12** 236–261

Gibson, M. M. and Launder, B. E. 1976. On the calculation of horizontal, turbulent, free shear flows under gravitational influence. *J. Heat Transfer*, **114**, 598–606

Gibson, M. M. and Launder, B. E. 1978. Ground effects on pressure fluctuations in the atmospheric boundary layer. *J. Fluid Mech.*, **86**, 491–511

Kasagi, N., Tomita, Y., and Kuroda, A. 1992. Direct numerical simulation of passive scalar field in a turbulent channel flow. *J. Heat Mass Transfer*, **114**, 598–606

Kim, J. and Moin, P. 1987. Transport of passive scalars in a turbulent channel flow. *Proc. 6th Symposium on Turbulent Shear Flows*, 5.2.1–5.2.6

Nagano, Y. and Kim, C. 1988. A two-equation model for heat transport in wall turbulent shear flows. *J. Heat Mass Transfer*, **110**, 583–589.

Park, T. S. and Sung, H. J. 1995. A nonlinear low-Reynolds-number k–ϵ model for turbulent separated and reattaching flows—I. Flow-field computations. *Int. J. Heat Mass Transfer*, **38**, 2657–2666.

Pope, S. B. 1983. Consistent modeling of scalars in turbulent flows. *Phys. Fluids*, **26**, 404–408

Reynolds, A. J. 1975. The prediction of turbulent Prandtl and Schmidt numbers. *Int. J. Heat Mass Transfer*, **18**, 1055–1069

Rogers, M. M., Mansor, N. N., and Reynolds, W. C. 1989. An algebraic model for the turbulent flux of a passiv scalar. *J. Fluid Mech.*, **203**, 77–101

Rubinstein, R. and Barton, J. M. 1990. Nonlinear reynolds stress models and the renormalization group. *Phys. Fluids*, **2**, 1472–1476

Speziale, C. G. 1991. Analytical methods for the development of Reynolds-stress closures in turbulence. *Ann. Rev. Fluid Mech.* **23**, 107–157

Vogel, J. C. and Eaton, J. K. Combined heat transfer and fluid dynamic measurements downstream of a backward-facing step. *J. Heat Mass Transfer*, **107**, 922–929

Youssef, M. S., Nagano, Y., and Tagawa, M. 1992. A two-equation heat transfer model for predicting turbulent thermal fields under arbitrary wall thermal conditions. *Int. J. Heat Mass Transfer*, **35**, 3095–3140